Agricultural Water Management 245 (2021) 106584

Contents lists available at ScienceDirect

Agricultural Water Management

journal homepage: www.elsevier.com/locate/agwat

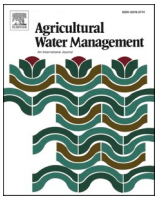

Research Paper

The feasibility of hand-held thermal and UAV-based multispectral imaging for canopy water status assessment and yield prediction of irrigated African eggplant (*Solanum aethopicum L*)

Paul Reuben Mwinuka [a,*], Boniface P. Mbilinyi [a], Winfred B. Mbungu [a], Sixbert K. Mourice [b], H.F. Mahoo [a], Petra Schmitter [c]

[a] *Sokoine University of Agriculture, Department of Engineering Sciences and Technology, Tanzania*
[b] *Sokoine University of Agriculture, Department of Crop Science and Horticulture, Tanzania*
[c] *International Water Management Institute (IWMI), Sri Lanka*

ARTICLE INFO

Handling Editor - Dr. B.E. Clothier

Keywords:
African eggplant
Crop water stress index
Irrigation
Remote sensing
Thermal imaging
UAV
Vegetation indices

ABSTRACT

This study was conducted to evaluate the feasibility of a mobile phone-based thermal and UAV-based multispectral imaging to assess the irrigation performance of African eggplant. The study used a randomized block design (RBD) with sub-plots being irrigated at 100% (I100), 80% (I80) and 60% (I60) of the calculated crop water requirements using drip. The leaf moisture content was monitored at different soil moisture conditions at early, vegetative and full vegetative stages. The results showed that, the crop water stress index (CWSI) derived from the mobile phone-based thermal images is sensitive to leaf moisture content (LMC) in I80 and I60 at all vegetative stages. The UAV-derived Normalized Difference Vegetation Index (NDVI) and Optimized Soil Adjusted Vegetation Index (OSAVI) correlated with LMC at the vegetative and full vegetative stages for all three irrigation treatments. In cases where eggplant is irrigated under normal conditions, the use of NDVI or OSAVI at full vegetative stages will be able to predict eggplant yields. In cases where, eggplant is grown under deficit irrigation, CWSI can be used at vegetative or full vegetative stages next to NDVI or OSAVI depending on available resources.

1. Introduction

Over the years, soil- and plant canopy-based methods have been employed for managing water in irrigated agriculture. Soil-based methods use either manual or computerized soil moisture monitoring technologies (Enciso et al., 2009; Zotarelli et al., 2011; Soulis et al., 2015). The use of soil moisture sensors provide point based soil moisture values and are sensitive to installation, calibration and location in the field. Depending on the density of soil moisture sensors, one might fail to capture field heterogeneity. Plant canopy-based methods have been recommended in recent years in crop water status monitoring because signs of canopy stress occur much earlier than soil-based signs (Poblete-Echeverría et al., 2017; Petrie et al., 2019). Canopy based methods are categorized into contact and non-contact measurements. Contact methods include the stomatal conductance and water potential measurements using ventilated and pressure chambers among others (Boyer, 1967; Goulden and Field, 1994). Examples of non-contact methods are infrared thermometers, mobile phone-based thermal imaging and remote sensing (Stone et al.; 2016; Reyes-González et al., 2018). The latter have been recommended due to their ability to indicate the plant physiological condition and leaf moisture content (LMC) throughout crop growth stages without interference leading to improved irrigation decisions (Zhang and Zhou, 2019). Depending on the sensor type and resolution, remote sensing methods, have the capability of indicating spatial variation of plant condition across the field. This helps the irrigator to apply water only in stressed zones. However, accuracy depends on the resolution of the images and the sensor used.

Mobile phone-based thermal imaging as part of non-contact methods, have been adopted due to its ability to indicate variations in canopy temperature within the plant canopy as a result of differences in leaf water content. As the leaf water content is related to the plant water availability in the soil, the canopy temperature and therefore leaf water content is dependent on the level of watering within the field. Well-watered plants have a high leaf water content resulting into low

* Corresponding author.
E-mail address: reubenpal@sua.ac.tz (P.R. Mwinuka).

https://doi.org/10.1016/j.agwat.2020.106584
Received 14 May 2020; Received in revised form 1 October 2020; Accepted 5 October 2020
Available online 31 October 2020

canopy temperature due to higher levels of transpiration from the plant stomata (Gusso, 2018). As water-stress causes stomatal closure, there will be a considerable reduction in transpiration leading to an increase in leaf surface temperature (DeJonge et al., 2015; Çolak et al., 2015). The crop water stress index (CWSI), a relationship between the canopy temperature for well-watered and stressed crops has been used to determine irrigation scheduling (Gerhards et al., 2016; Grant et al., 2016). The use of mobile phone-based thermal imaging has worked well in the computation of crop water stress indices with variation in effectiveness depending on crop type and climatic conditions. Whilst the method has been found useful at plant level, it is labor intensive to capture the heterogeneity in farmer fields.

Remote sensing images from satellites, aircraft and unmanned aerial vehicles (UAV) provide valuable information for agricultural decision making (Ballester et al., 2019; Jorge et al., 2019; Siegfried et al., 2019). Among these methods, UAVs have been recommended in agricultural water management because of its ability to collect high-resolution data at low-cost without cloud interference (Alvino and Marino, 2017). The UAVs carry sensors of different types such as visual, thermal, multispectral or hyperspectral with varying sensitivity depending on the applications. Multispectral sensors collect information in three to ten broadband reflectance while hyperspectral bands collect information from hundreds of narrow-band reflectance (Badzmierowski et al., 2019; Zhang and Zhou, 2019). Vegetation indices (VI), derived by calculating the ratios of two or more spectral bands, vary in function of canopy moisture content as different level of plant water status results in different spectral responses. For instance, well-watered plant canopy is characterized by a high reflectance of near infrared (NIR) and low reflectance of red bands (Genc et al., 2013; Van Beek et al. 2013). Hence, different vegetation indices can be derived to assess plant water status. Stone et al. (2016) and Reyes-González et al. (2018) recommended the use of normalized difference vegetation index (NDVI) in delineating water-stressed zones within a corn field. Likewise, studies under turf grass systems, recommended the use of NDVI and green-to-red ratio index (GRI) in the estimation of soil moisture status (Badzmierowski et al., 2019). Jorge et al. (2019) recommended normalized difference red-edge (NDRE) among other vegetation indices due to its capability of detecting water-stressed zones in olive trees. This is due to the sharp response of the reflectance between the red and NIR spectral bands with water stress. Additionally, Shi et al. (2019) suggested the use of soil adjusted vegetation index (SAVI) and NDVI in identifying field spatial variability as they strongly correlate with the CWSI.

Furthermore, vegetation indices derived from NIR and red spectral bands, can be used in crop yield prediction (Katsoulas et al., 2016). Kyratzis et al. (2017) recommended the use of GNDVI and NDVI to predict durum wheat yield subjected under water stress in the Mediterranean environment. Similarly, Ballester et al. (2019) recommended the NDVI in forecasting cotton yield in semi-arid environments. Likewise, Ihuoma and Madramootoo (2019) recommended the combination of the water index (WI) and NDVI to assess water stress impacts on bell pepper yield. Furthermore, Maresma et al. (2016) suggested the use of various vegetation indices such as Wide Dynamic Range Vegetation Index (WDRVI) for assessing maize yield.

Vegetation indices maps are an alternative to productivity maps to support targeting of agricultural water management interventions (Veysi et al., 2017). The maps convert numerical values of vegetation indices into color scales depicting water stressed zones to support quick evaluations. Different vegetation indices maps such as NDRE, GNDVI and NDVI have been used due to their capability of mapping the variation of water supply within a field (Shiratsuchi et al., 2011; Genc et al., 2013; Damian et al., 2020). So far studies focus predominantly on staple crops such as maize and few measure the interaction between fertilizer application and deficit irrigation rates on crop yield (Shiratsuchi et al. 2011; Stone et al., 2016).

Despite the potential of mobile phone-based thermal and UAV-based multispectral vegetation indices in assessing crop water stress in various crops, their application for vegetables, grown under deficit irrigation, is limited. Little information is found on the ability of vegetation indices to depict crop water stress in vegetables (e.g. African eggplant) under drip systems using deficit irrigation in tropical sub-humid areas. Each crop has different spectral response due to differences in climatic conditions, leaf structure, water stress levels and plant water uptake response functions influencing leaf water composition (Bellvert et al., 2014). Establishing UAV or mobile phone-based thermal imagery assessments to assess irrigation performance for irrigated crops such as African eggplants can support public or private sector extension services for small, medium and large scale farming. As part of Tanzania's economic growth development strategy (Mandalu and Costa, 2018; Wuyts and Kilama, 2014) small scale farming is expected to shift to large scale farming as a result of increasing demand of food and raw materials for industrial development. Management of large scale farms or contract farming of smallholders will require the development of contextually relevant advisory services to enhance yields and water-use efficiency.

Therefore, this study aimed at investigating the efficacy of using the crop water stress index (CWSI) and vegetation indices (VI) in assessing irrigation performance of African eggplant under different irrigation strategies in a tropical sub-humid area. Specifically, the study aimed at using mobile phone-based thermal imaging and UAV derived multispectral imaging to: (1) evaluate whether LMC, CWSI and VI differ at different irrigation depths throughout cropping stages; * investigate the sensitivity of the CWSI and vegetation indices to LMC variation among irrigation treatments; (3) develop vegetation indices maps to capture spatial and temporal variations in irrigation application and support precision agriculture; and (4) assess the applicability of CWSI and vegetation indices to predict crop yield.

2. Materials and methods

2. 1 Description of the study site

The study was conducted at Rudewa watershed in Kilosa District within Morogoro Region in Tanzania. The watershed lies between 6°32′ to 6°47′South and 36°8′ to 37°28′East with an average altitude of 437 m above mean sea level (Fig. 1). The average annual temperature of the study site is between 15.1 °C and 24.4 °C and the mean relative humidity around 67.5%. The minimum average temperature of 12.9 °C is recorded in July while the maximum average temperature of 32.1 °C is recorded in February. The site is characterized by a bimodal rainfall regime with an average annual rainfall between 1000 mm and 1400 mm. The short rains occur from October to December and long rains from March to May. Most of the agricultural activities are rainfed with rice and maize being the major food crops during the long rainy period. However, during the dry period (June to October) and short rainy period (December to February), full or supplemental irrigation is required for crops like African eggplant and tomato.

The major source of irrigation water is the Wami River, a perennial river originating from the Mamiwa Forest Reserve. The study site has sand clayey loamy soils with a medium level of organic carbon. The clay, silt and sand content range between 23% and 26%, 10–14% and 58–65% respectively within the top 40 cm soils. The average soils bulk density within the study sites is 1.3–1.5 g/cm^3.

2. 2 Experimental design, irrigation water requirements and the actual irrigation

The experiment was conducted using a randomized block design (RBD) with 3 irrigation application rates: 100% (I100), 80% (I80) and 60% (I60) of crop water requirements and 3 replicates per treatment (Fig. 2). Nitrogen fertilizer was uniformly applied at a rate of 250 kg/ha (i.e. 100%) for all treatments and was part of a larger study as described in Mwinuka et al. (in press).

Crop water requirements were estimated using CROPWAT 8.0

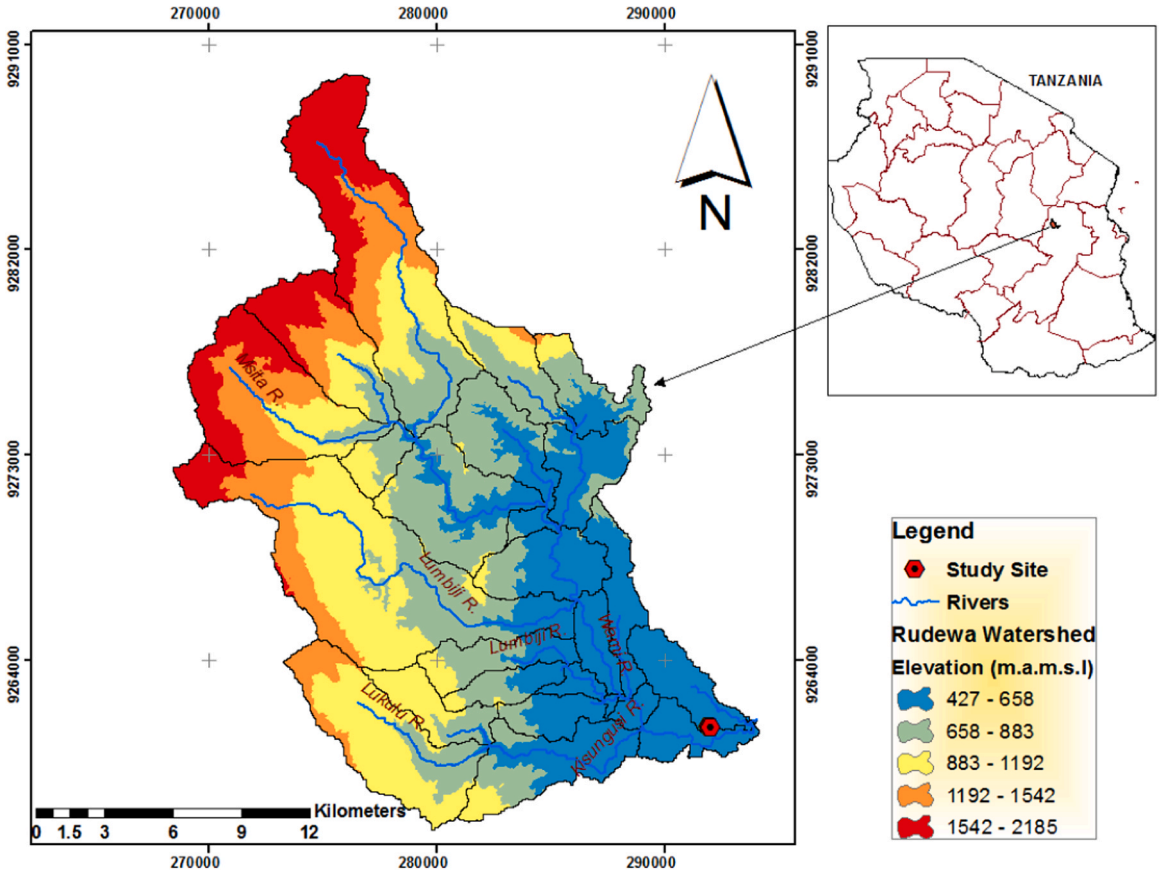

Fig. 1. The watershed of the study site, Rudewa village in Kilosa – Morogoro region, Tanzania (Source: Mwinuka et al., in press).

Fig. 2. Experimental plot with irrigation application at 100% (I100), 80% (I80) and 60% (I60) of calculated crop water requirements.

Table 1
Crop evapotranspiration and irrigation water requirements at different cropping stages.

Month	Stage	Kc coefficient	ETo (mm/day)	ETc (mm/day)	Effective rain (mm)	IWRn (mm/day)	GIWR (mm/day)
June	Early	0.6	3.4	2	0	2	2.4
July	Vegetative	0.7	3.4	2.4	0	2.4	2.8
July	Full vegetative	1.1	3.4	3.7	0.1	3.6	4.2
August	Full vegetative and late-season	1.1	3.7	4.1	0	4.1	4.8
September	Late-season	1.1	4.3	4.7	0	4.7	5.5
October	Late-season	1	4.9	4.9	0.2	4.7	5.5

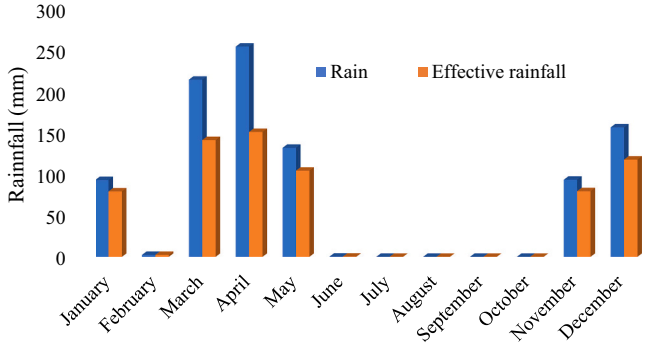

Fig. 3. The average monthly rains for the 2017 and 2018 cropping seasons.

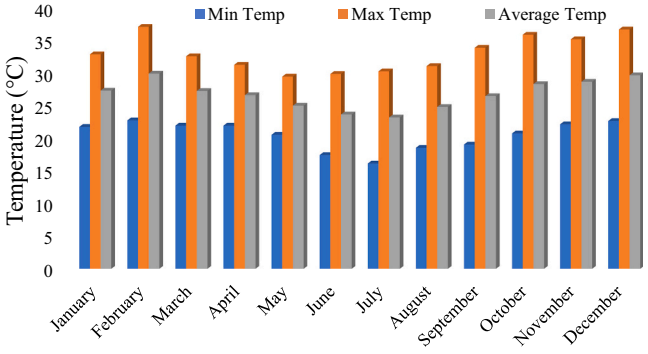

Fig. 4. The average monthly temperature for the 2017 and 2018 cropping seasons.

software as recommended by FAO (Diku et al., 2015) using 15 years of climatic data from Ilonga meteorological station. The crop actual evapotranspiration (ETc) was estimated using the crop coefficient (Kc) and crop reference evapotranspiration (ETo). The ETo was calculated using a FAO CLIMWAT 2.0 software (Diku et al., 2015). Furthermore, the estimated daily net irrigation water requirements (IWRn) and gross irrigation requirements (GIWR) were calculated (Table 1). The water application and conveyance efficiencies of the system were 94% and 90% which was estimated from the relationship of the dripline discharge and the total volume of water supplied.

Subsequently, microclimate data were used to fine-tune daily water requirement through an automatic weather station installed adjacent to the experimental plot. Within the two cropping seasons (June to October of 2017 and 2018) the average rainfall, effective rainfall and temperature for the study site were recorded (see Figs. 3 and 4). The effective rainfall was estimated by USDA-SCS method as described by Patwardhan et al. (1990) but found too low to be significantly contributing to the crop water balance.

Irrigation water was applied through non pressurized drip lines. The irrigation application was regulated through a water control valve installed in each sub-main line. Irrigation was activated when soil moisture reached the maximum allowable depletion (i.e. 17% volumetric soil moisture content). The amount of water irrigated for each treatment was measured using an installed flow meter (Table 2).

2. 3 Data collection throughout the irrigation season

2.3. 1 Soil and plant canopy moisture measurements

Soil sampling was conducted by establishing five sampling quadrants of 5 × 5 m to represent the field. From each quadrant, five sampling points were marked where undisturbed soil samples were taken using 100 cm^3 metallic cylinders. Soil samples were taken at a depths 0–20 and 20–40 cm in representative locations at the beginning of the cropping season. Samples were analysed for field capacity (FC) and permanent wilting point (PWP) using a pressure plate apparatus at a soil matric suction of 30 kPa and 1500 kPa respectively. The average volumetric FC and PWP moisture content was 28% and 14%. Soil moisture was measured from six measuring points in each treatment. Moisture measurements were conducted using a calibrated DSMM500 soil moisture sensor every 24 h between irrigation. The sensor detects soil moisture to a depth of 20 cm.

Moisture content from the plant leaves was taken through the irrigation cycle in all treatments. To minimize solar radiation errors caused by evaporation, leaves were harvested between 08:00 and 10:00 h. The fresh weight (Wl) samples were recorded and dried in the greenhouse to prevent samples from deterioration. Samples were finally oven-dried at 70 °C until a constant weight (Dl) was attained. Leaf dry samples were then determined according to Ge et al. (2016) as shown in Eq. (1).

$$LWC = \frac{Wl - Dl}{Wl} \times 100\% \quad (1)$$

Table 2
The actual amount of water applied for different treatments at each crop development stage.

Treatment	Applied water (mm)				
	Initial stage	Development stage	Mid-season	Late season	Total
I100	50.2	58.7	102.5	824.5	1035.9
I80	40.2	47.0	82.0	659.6	828.8
I60	30.1	35.2	61.5	494.7	621.5

2.3. 2 Determining of the crop water stress index using mobile phone-based thermal imaging

Canopy temperature was collected by a FLIR camera (FLIRone camera P/N 435-0003-01-00) connected to Samsung Galaxy S5 smartphone. The FLIRone camera captures both thermal and visible spectrum. The sensor has a thermal resolution of 240 × 320 pixels and a temperature sensitivity of 0.1 °C. Its scene temperature ranges between − 20 and 120 °C and operates at a temperature range of 0–35 °C. Additionally, an emissivity of 0.98 was used, a common emissivity value when estimating canopy temperature of horticultural crops (Chen, 2015; Gerhards et al., 2016; Xue and Su, 2017). Thermal images were acquired between 12:00 and 14:00 h from six monitoring plants in each plot throughout the season as mentioned by Grant et al. (2016). Thermal images were acquired throughout the irrigation cycle all subsequent days after irrigation so that to record the canopy temperature at different levels of soil moisture. FLIRone and FLIR-tools computer software (P/N 435-0003-01-00) were used to process thermal images. The canopy temperature (for instance sp1 to sp8 in Fig. 5) for water stressed treatments were higher as compared to non-stressed canopy with values ranging between 29.7 °C to 32 °C and 24.2 °C to 25.8 °C, respectively (Fig. 5A and B).

The crop water stress index (CWSI) was calculated from the relationship of canopy temperature (Tc), artificial wet reference temperature (Tw) and dry reference temperature (Td) according to (Levy et al., 2013; Baluja et al., 2012; Petrie et al., 2019) as shown by Eq. (2).

$$CWSI = \frac{Tc - Tw}{Td - Tw} \quad (2)$$

The canopy temperature for each treatment was estimated from the temperature images acquired by a FLIRone camera. The average pure canopy temperature (T_c) was obtained by eliminating the soil background surface using the thermal fusion and box tool within the FLIR-tools computer software (version 5.9.16284.1001). Reference artificial wet temperature (T_w) was estimated using the manual aspirated psychrometer (Psychron 15691) (Yonah et al., 2018). The canopy dry reference temperature (T_d) was simulated by covering the leaf by petroleum jelly to prevent it from transpiration, a condition of non-transpiring canopy (Poblete-Echeverría et al., 2017; Jones et al., 2002).

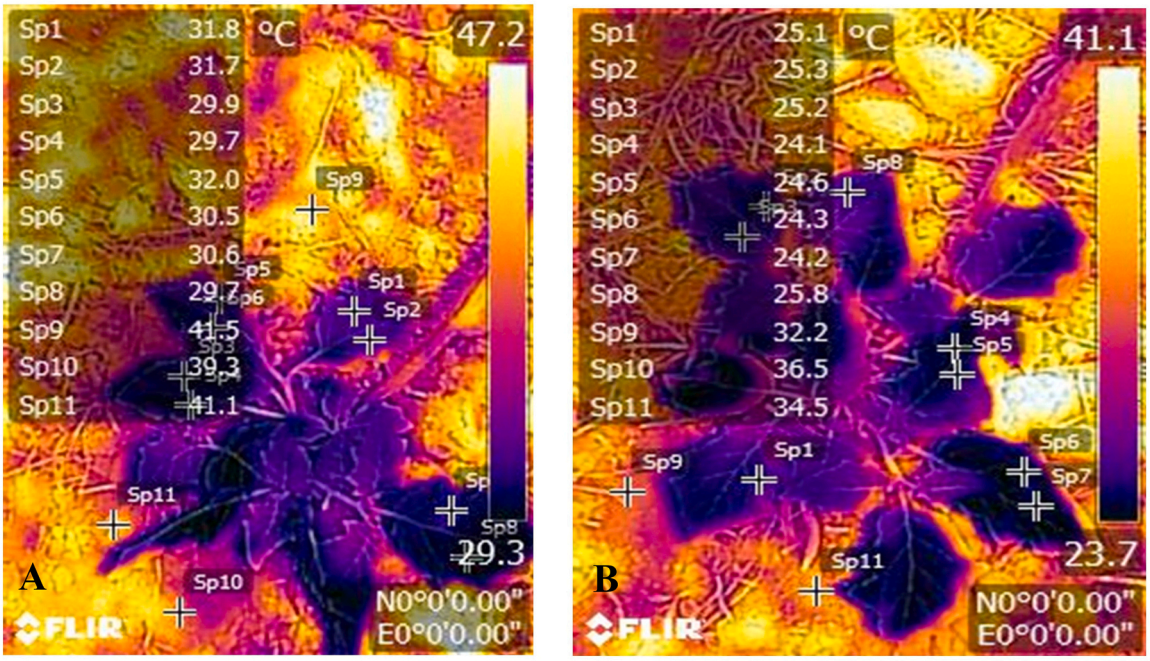

Fig. 5. Thermal imagery temperature variation on canopy (Sp1 to Sp8) and on soil surface (Sp9 to Sp11) under water stressed (A) and non-stressed conditions (B).

2. 4 Determining vegetation indices using UAV derived multi-spectral bands

2.4. 1 UAV images acquisition

Images were acquired using a multispec4c sensor attached to the fixed wings UAV eBeeTM drone (a senseFly SA, Cheseaux-Lausanne, Switzerland). The fields were georeferenced using a global positioning system (GPS). The points were then recorded in a csv file format and processed using QGIS 2.18 to produce a kml file. The kml files were imported in the eMotion 3 computer software for the creation of flight plans.

The multispec4c sensor had four spectral bands (green, red, red edge and near-infrared). The corresponding wavelengths for the respective spectral band was 550 nm, 660 nm, 735 nm and 790 nm. The sensor was set at 1.2 Megapixel providing a full resolution of 12 cm/pixel with a lateral and longitudinal overlap of 70% and 65%. The images were taken between 12:00 and 13:30 h to minimize the effects of shadow using a UAV flown at an average altitude of 115 m above elevation data (AED). Radiometric calibration of the sensor was conducted before each flight using a calibration board.

Table 3
Vegetation indices used in the assessment of canopy water status.

Index	Equation	Reference
Green-Red Vegetation Index	$GRVI = \frac{G-R}{G+R}$	Xue and Su, 2017
Normalized Difference Vegetation Index	$NDVI = \frac{NIR-R}{NIR+R}$	Ustuner et al., 2014
Green Normalized Difference Vegetation Index	$GNDVI = \frac{NIR-G}{NIR+G}$	Omer et al., 2017
Normalized Difference Red Edge	$NDRE = \frac{NIR-RE}{NIR+RE}$	Ustuner et al., 2014
Enhanced Vegetation Index	$EVI2 = 2.5(\frac{NIR-R}{NIR+2.4R+1})$	Picoli et al., 2017
Soil Adjusted Vegetation Index	$SAVI = \frac{1.5(NIR-R)}{NIR+R+0.5}$	Mulla, 2013
Optimized Soil Adjusted Vegetation Index	$OSAVI = \frac{(NIR-R)}{NIR+R+0.16}$	Zou and Mõttus, 2017
Transformed Difference Vegetation Index	$TDVI = \sqrt{0.5+\frac{NIR-R}{NIR+R}}$	Xue and Su, 2017

2.4. 2 UAV images processing and computation of vegetation indices

Production of digital surface model (DSM) orthomosaic maps from multispectral images was conducted using the SenseFly PIX4D software. The processed orthomosaic maps were trimmed to the field level using the extraction clipper application in the QGIS 2.18 software. A geometric correction process (image to image registration) was conducted to ensure that images for each of the treatments corresponded to the same location throughout the irrigation cycle (Dave et al., 2015). Images in different spectral bands were extracted using a python script and used to compute different vegetation indices through raster and rgdal packages in R software (version 3.6.1) (Table 3). Soil background effect were corrected by setting a vegetation index threshold value which separates bare soil surface from vegetation (Naji, 2018). The decision of the threshold values to use was considered after studying the values of vegetation indices from the bare soil and the soil with vegetation cover. The choice of vegetation indices was based on their capability to capture variations in the canopy leaf water content (Katsoulas et al., 2016; Stone et al. 2016; Jorge et al., 2019) and were limited to four spectral bands (green (G), red (R), near-infrared (NIR) and red edge (RE)) available in multispec4c sensor (Table 3).

2. 5 Data analysis and statistics

The sensitivity of CWSI and other vegetation indices (VI) to LMC in different irrigation depths at various cropping stages was assessed using the analysis of variance (ANOVA) test. CWSI and VI which showed a significant difference among the different irrigation treatments ($p < 0.05$) were selected and their correlation with LMC was explored. The analyses were performed using R software (version 3.6.1). Vegetation indices maps were developed to assess spatial variation in plant water status within the different drip treatments. The image mosaic was processed using the rgdal and raster packages for evaluating the vector spatial data in the respective bands through Rstudio (version 3.6.1) software. The plot function was applied to generate vegetation indices

Table 4
The ANOVA table for different variables at different irrigation depth applied .

	LMC	CWSI	GNDVI	GRVI	SAVI	NDVI	OSAVI	EVI2	NDRE	TDVI
Early development stage										
I100	***	*	NS	NS	NS	NS	NS	NS	NS	NS
I80	***	***	NS	NS	NS	NS	NS	NS	NS	NS
I60	***	***	NS	NS	NS	NS	NS	NS	NS	NS
Vegetative stage										
I100	***	NS	NS	**	**	*	*	NS	*	NS
I80	***	*	***	NS	**	**	**	NS	NS	NS
I60	***	***	NS	**	NS	***	***	NS	NS	NS
Full vegetative stage										
I100	***	NS	NS	**	NS	***	***	NS	NS	NS
I80	***	***	NS	NS	*	**	**	NS	NS	NS
I60	***	***	NS	**	*	**	**	NS	NS	NS

*, ** and *** refer to signficance levels 0.05, 0.01 and 0.001, NS = not significant

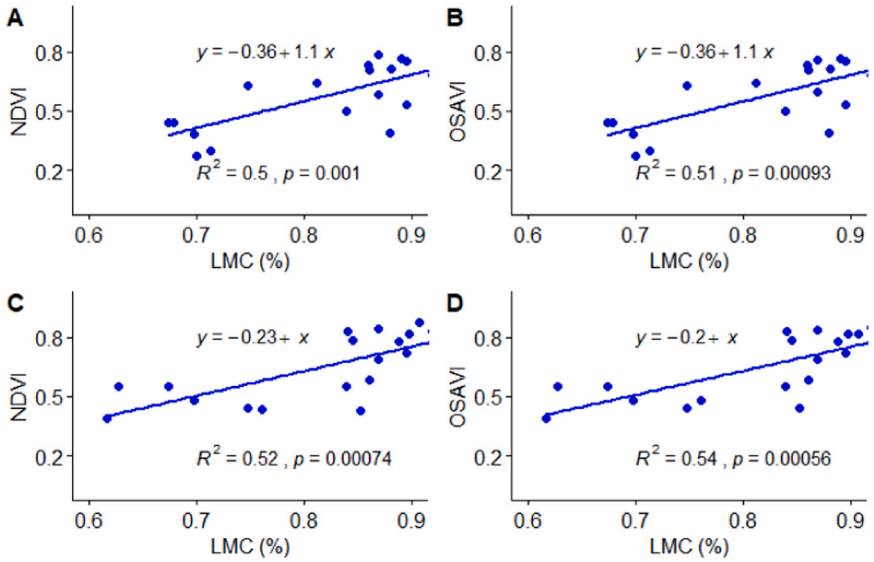

Fig. 6. The relationship between the vegetation indices with LMC for fields irrigated at I100 during vegetative (A and B) and full vegetative (C and D) crop development stages.

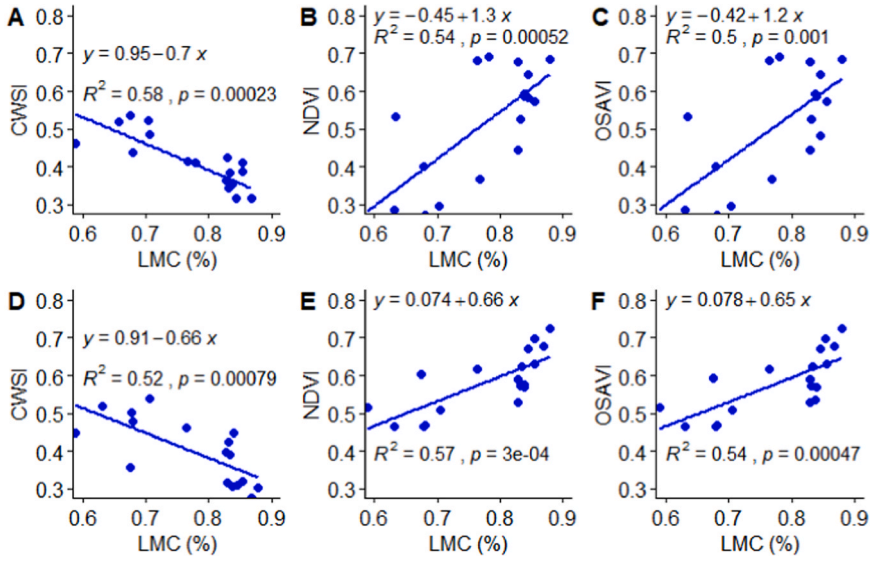

Fig. 7. The relationship between the vegetation indices with LMC for fields irrigated at I80 during early (A), vegetative (B and C) and full vegetative (D, E and F) crop development stages.

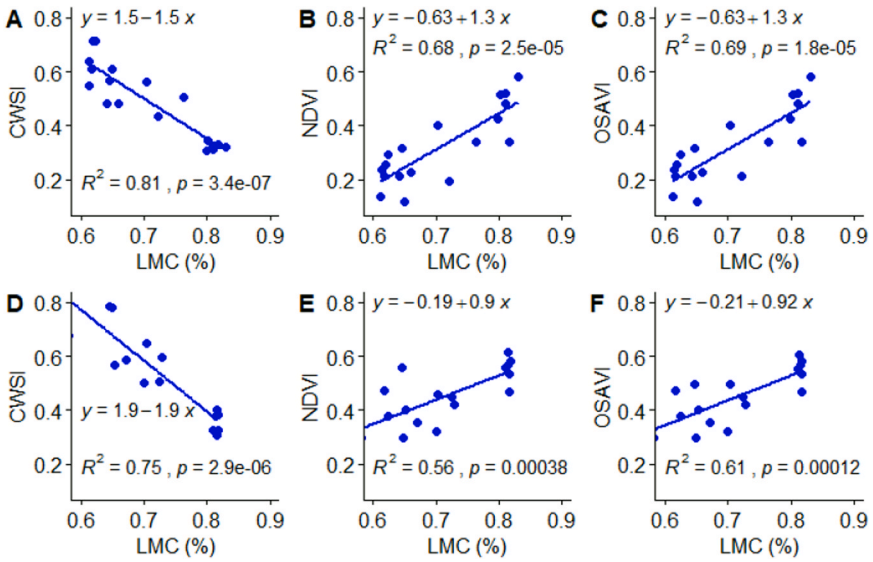

Fig. 8. The relationship between the vegetation indices with LMC for fields irrigated at I60 during vegetative (A, B and C) and full vegetative (D, E and F) crop development stages.

maps.

Yield prediction was conducted by developing a linear regression model between the vegetation indices with the first season yields. The second season yields were used to test the accuracy of the model by developing a regression relationship of the predicted and observed yields. The root mean square error (RMSE) was then calculated to show the yield prediction error of vegetation indices at different treatments (Zhao et al., 2020). Yield prediction was conducted through ggplot2 and ggpubr packages under Rstudio (version 3.6.1) software. The vegetation indices with the coefficient of determination greater than 0.5 was considered sensitive in forecasting the end of the season yields.

3. Results

3. 1 The response of the LMC, CWSI and VI to irrigation treatment

The LWC, CWSI and vegetation indices responded differently at different irrigation rates within the irrigation cycle (Table 4). The LMC was significantly different in all treatments at early, vegetative and full vegetative stages ($p < 0.001$). Similar results were obtained for CWSI except at highest irrigation rates (I100) during the vegetative and full vegetative stages. From all the VI measured, the GNDVI responded well at I80 during the vegetative stage ($p < 0.001$) but not for other irrigation treatments or in other stages. The NDVI and OSAVI were able to pick up differences in LMC across all water treatments during the vegetative and full vegetative stages. In contrast, the EVI2, TDVI and NDRE had a weak response to irrigation applied across all cropping stages.

3. 2 The sensitivity of CWSI and VI to LMC in different irrigation treatments

The CWSI and VI responded differently to LMC at all three crop development stages. At I100, the correlation of NDVI and OSAVI with LMC was 0.5 and 0.51, during the vegetative stage, and 0.52 and 0.54, during the full vegetative stage, respectively (Fig. 6). For I80, the correlation between CWSI and LMC was 0.58 at early crop stage (Fig. 7). During the vegetative stage, the correlation with LMC was 0.54 and 0.5 for the NDVI and OSAVI. At full vegetative stage, the CWSI, NDVI and OSAVI correlation with LMC was 0.52, 0.57 and 0.54, respectively.

At 60% of irrigation depth, the CWSI, NDVI and OSAVI during the vegetative stage were 0.81, 0.68 and 0.69 (Fig. 8). This reduced slightly during the full vegetative stages of crop development.

Other vegetation indices, responded well in some occasions (figures not shown). For example, the GNDVI responded well to leaf moisture content to I80 ($r^2 = 0.52$, $p = 0.0006$) at the vegetative stage. The GRVI responded well in detecting the LMC ($r^2 = 0.63$, $p = 8.3 \times 10^{-5}$) at I60 during the full vegetative stage of crop development. On the other hand, SAVI had a weak response in all development stages despite the occurrence of significant differences among treatments.

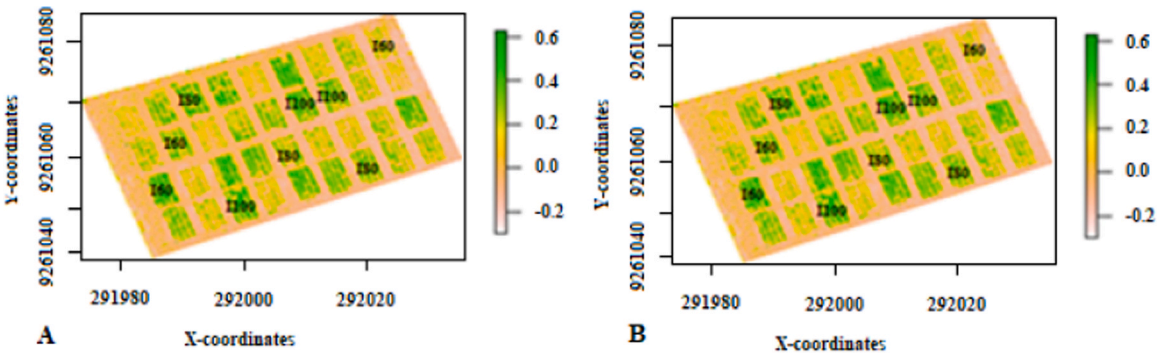

Fig. 9. NDVI (A) and OSAVI (B) at vegetative stage of crop development.

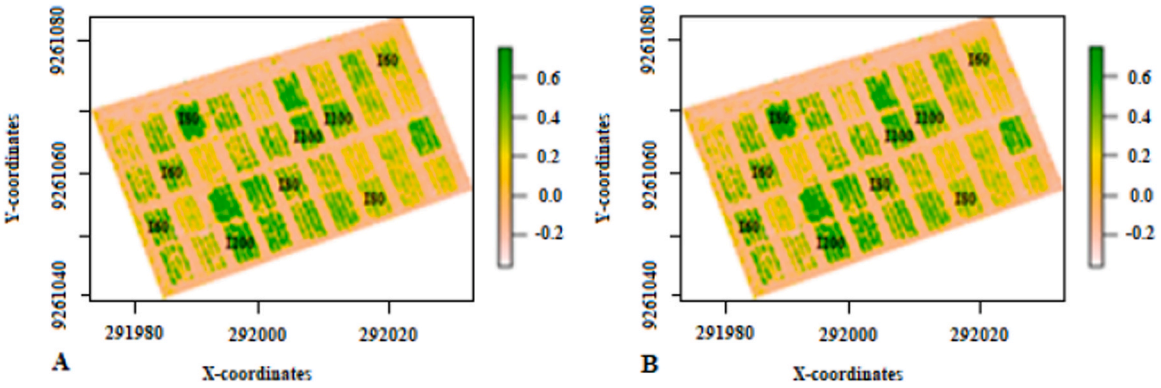

Fig. 10. The NDVI (A) and the OSAVI (B) at full vegetative stage of crop development.

3. 3 Mapping of vegetation indices for spatial field water status assessments

As mentioned in the previous sections, both the NDVI and the OSAVI outperformed the other selected VI in assessing LMC changes as a result of the irrigation treatment. Hence, NDVI and OSAVI were used to assess the in-field spatial variation and the difference in irrigation treatment. At the vegetative stage (40 days after transplanting), the NDVI and OSAVI ranged between − 0.3 to 0.62 and − 0.32 to 0.6, respectively with most of negative values representing areas with bare soils (Fig. 9). Areas where water stress occurred, and influenced crop performance, typically ranged between 0.2–0.35 and 0.2–0.32. Differences in these vegetation indices were caused by different irrigation treatments applied within the field and uniformity issues among certain drip lines.

During the full vegetative stages (60 days after planting), the NDVI was in the range of − 0.3 to 0.74 and OSAVI in the range of − 0.35 to 0.72 (Fig. 10). Water stressed areas, influencing crop performance, typically ranged between 0.3 and 0.4 for both NDVI and OSAVI.

3. 4 Yield prediction using CWSI and vegetation indices

The average fruit yields for I100, I80 and I60 were 63 t/ha, 51.1 t/ha and 43.1 t/ha and differed significantly among the three treatments ($p < 0.001$). The results showed that the I80 treatment resulted in a higher water use efficiency and was defined as an optimum irrigation strategy under water limiting conditions (see details in Mwinuka et al. (in press)). The CWSI for the I80 treatment at vegetative and full vegetative stages was 0.44 ± 0.14 and 0.39 ± 0.08, respectively (Table 6). The corresponding NDVI and OSAVI was 0.44 ± 0.2 and 0.53 ± 0.1. At the full vegetative stage, the CWSI, NDVI and OSAVI was 0.39 ± 0.08, 0.58 ± 0.08 and 0.58 ± 0.08, respectively. The indices for I100 and I60 are indicated in Table 6.

The ability to predict yield at vegetative and full vegetative stages depended on the index used (Table 5). At the vegetative stage, the use of CWSI enabled the prediction of eggplant yields in the I60 treatment ($r^2 = 0.53$). Predicting eggplant yields using CWSI was possible using data in either the vegetative or the full vegetative stage in the I80 treatment. As plants were not stressed under I100, the use of CWSI did not result in a

Table 5
Mean vegetation indices and yield prediction for eggplant under different irrigation treatments.

Treatment	CWSI					NDVI					OSAVI				
	Mean	SD	Model	r^2	p	Mean	SD	Model	r^2	p	Mean	SD	Model	r^2	p
Vegetative stage															
I100	0.23	0.07	NS	NS	NS	0.56	0.14	y = 43 + 36x	0.60	0.014	0.56	0.14	y = 42 + 37x	0.57	0.018
I80	0.44	0.14	NS	NS	NS	0.44	0.2	y = 23 + 51x	0.73	0.0034	0.53	0.10	y = 39 + 27x	0.69	0.0053
I60	0.49	0.2	y = 58–33x	0.53	0.026	0.32	0.14	y = 39 + 18x	0.64	0.0095	0.32	0.14	y = 39 + 18x	0.63	0.01
Full vegetative stage															
I100	0.30	0.09	NS	NS	NS	0.62	0.14	y = 51 + 21x	0.38	0.076	0.62	0.15	y = 51 + 21x	0.44	0.05
I80	0.39	0.08	y = 66–34x	0.55	0.022	0.58	0.08	y = 26 + 45x	0.76	0.0021	0.58	0.08	y = 28 + 42x	0.71	0.004
I60	0.61	0.16	y = 56–19x	0.76	0.0022	0.45	0.10	y = 25 + 39x	0.56	0.02	0.44	0.10	y = 24 + 42x	0.59	0.015

SD = Standard deviation, x = vegetation indices, y = yield (t/ha), NS = non significant at $p < 0.05$

Table 6
Yield model performance based on CWSI, NDVI and OSAVI at vegetative and full vegetative stages.

Treatment	CWSI			NDVI			OSAVI		
	RMSE[a]	r^2	p	RMSE	r^2	p	RMSE	r^2	p
Vegetative stage									
I100	NS	NS	NS	2.82	0.67	0.0072	2.96	0.69	0.0054
I80	NS	NS	NS	5.99	0.77	0.0019	5.09	0.71	0.0045
I60	2.9	0.62	0.011	3.58	0.63	0.011	3.45	0.65	0.009
Full vegetative stage									
I100	NS	NS	NS	NS	NS	NS	NS	NS	NS
I80	3.93	0.78	0.0016	2.77	0.87	0.00027	2.77	0.86	0.00033
I60	3.32	0.6	0.015	2.15	0.54	0.025	2.07	0.57	0.019

[a] Root mean square error (RMSE) in t/ha.

good prediction model. At the full vegetative stage, yield prediction could be derived for I80 or I60 using either CWSI (I80: $r^2 = 0.55$; I60: $r^2 = 0.76$), NDVI (I80: $r^2 = 0.76$; I60: $r^2 = 0.56$) or OSAVI (I80: $r^2 = 0.71$; I60: $r^2 = 0.59$) (Table 5).

The established regression models were validated using the eggplant yields from the second season. The performance of the CWSI, NDVI and OSAVI based yield prediction models varied amongst irrigation treatments and depended on the crop stage (Table 6). Except for I100, OSAVI based prediction models seemed to result in a slightly lower RMSE compared to those using NDVI. Furthermore, for NDVI and OSAVI based predictions, RMSE improved when using data from the full vegetative stage. For I80, the use of the NDVI ($r^2 = 0.87$, RMSE = 2.77 t/ha) and the ODVI ($r^2 = 0.86$, RMSE = 2.77 t/ha) at the full vegetative stage performed better than CWSI ($r^2 = 0.78$, RMSE = 3.93 t/ha). For I60, at the vegetative stage, the yield predictions using CWSI ($r^2 = 0.62$, RMSE = 2.9 t/ha) outperformed those derived using NDVI ($r^2 = 0.63$, RMSE = 3.58 t/ha) and OSAVI ($r^2 = 0.65$, RMSE = 3.45 t/ha) (Table 6). Whilst at the full vegetative stage using OSAVI ($r^2 = 0.57$, RMSE = 2.57 t/ha) resulted in slightly better yield predictions compared to CWSI ($r^2 = 0.6$, RMSE = 3.32 t/ha) and NDVI ($r^2 = 0.54$, RMSE = 2.15 t/ha) (Table 6).

4. Discussion

The leaf moisture content (LMC), crop water stress index (CWSI) and vegetation indices (VI) differed significantly at different irrigation regimes. The CWSI was significantly different to I80 and I60 water regimes within the irrigation cycle. These differences were caused by a significant rise of temperature within the plant canopy as the canopy moisture content decreases (DeJonge et al., 2015; Çolak et al., 2015; Prashar and Jones, 2014). Furthermore, the highest canopy temperature was observed in the treatments leading to increased levels of water stress (i.e. I60), resulting in high correlation of CWSI to LMC within the irrigation cycle. Insignificant differences occurred at I100 was due to high accumulation of leaf moisture within the plant canopy and hence low variation of leaf temperature (Gusso, 2018).

Other vegetation indices had a different response to varying plant canopy moisture content. At early crop development, all vegetation indices were not significantly different. This is due to soil background interference as most of the reflectance was observed from the soil surface (Ballester et al., 2019). At vegetative and full vegetative cropping stages, various vegetation indices responded differently due to a difference in spectral response to the plant canopy. The NDVI and OSAVI differed significantly within the vegetative and full vegetative stages in all irrigation regimes. The GRVI and SAVI was sensitive only for some irrigation regimes. This indicates that, the NIR spectral response was more sensitive to the variation of canopy temperature as compared to the green band (Peng et al., 2013). Badzmierowski et al. (2019) reported a good response of NDVI to distinguish LMC across the field of turfgrass. On the contrary, the EVI2, TDVI and NDRE had a weak capability of differentiating leaf moisture content. The failure of NDRE is due to the weak response of the red-edge spectral band to variations in the leaf moisture content. This is contrary to the study conducted in irrigated maize fields (Siegfried et al., 2019) where the NDRE was capable of distinguishing differences in plant water stress. This is because, maize was sensitive to the red-edge reflectance due to its leaf greying with water stress resulting in a detectable signal by the sensor (Siegfried et al., 2019).

Moreover, the spatial variation as a result of irrigation treatment and inter drip-line uniformity was reflected in the NDVI and OSAVI based VI maps. The variation of the plant condition within the field as a result of the different levels of water application resulted in a different color scales. For instance, non-water stressed plants resulted in high NDVI and therefore green color whilst the water stressed plants in the I60 had lower values and a yellowish color. Also, Veysi et al. (2017) recommended the use of indices maps for spatial and temporal management of irrigation water in sugarcane production by distinguishing areas with high, medium and low water stress within the whole cropping season. More studies have shown the opportunity of using vegetation indices in mapping water deficiency in irrigated fields (Genc et al. 2013; Stone et al., 2016; Damian et al. 2020). The application of this technology in African eggplant production is anticipated to boost yields, increase water use efficiency but also reduce production cost through improved targeting of water and fertilizer application.

The reflection of the plant physiological status during the vegetative stages, as a result of water application, was reflected in eggplant yields. Hence, those indices which showed sensitivity to the LMC were able to predict eggplant yields. The CWSI, as a stress indicator, was able to better predict yields at 60% using the vegetative stage. This is likely due to the fact that the water stress in the vegetative stage correlated better with declines in yield than those observed in the full vegetative stage. For 80%, the water stress indicator in the full vegetative stage were found to be better yield predictors. The NDVI and OSAVI performed well in predicting yield at I100 as well as under water stressed conditions due to the high capability of detecting plant water stress responsible for yield declines. Siegfried et al. (2019) also observed a good correlation of OSAVI with maize yields at different soil moisture levels. Similarly, Ballester et al. (2019) recommended the use of NDVI as good predictors of lint yield as compared to others. Likewise, Ranjan et al. (2019) recommended the application of NDVI (r = 0.62), TDVI (r = 0.61), GNDVI (r = 0.54), SAVI (r = 0.62) and OSAVI (r = 0.62) to predict the pinto bean yields. The variation in the best performance of these indices depends on leaf size and plant mechanisms responsible for the adaptation to water stress. As this results in differences in canopy spectral reflectances in concordance to the LMC, indices therefore have different capabilities in predicting yields under deficit irrigation using drip.

5. Conclusion

Variation of leaf moisture content at different levels of irrigation enables canopy water stress assessments. It is important to understand not only the predictive ability of each of the VI but also its relation to the translation of water stress into plant physiology and crop yield which differs among crops, soil and climate conditions. This study compared various vegetation indices and CWSI to assess irrigation performance and detect water stress in African eggplant under deficit irrigation. As plant water stress results in increased canopy temperature, CWSI correlates well with LMC and can be used to predict yields under deficit irrigation. The response of vegetation indices derived from a UAV multispectral sensor, to LMC, varied depending on the spectral bands combined, the soil interference, and the cropping stage used. For example, during the early stages of the crop, vegetation indices responded poorly to LMC changes due to soil background reflectance interference. NDVI and OSAVI were the two best performing VI, correlating well with LMC changes, and predicting yields as affected by deficit irrigation under drip systems. In cases were eggplant is irrigated under normal conditions, the use of NDVI or OSAVI at full vegetative stages will be able to predict eggplant yields. In cases were, eggplant is grown under deficit irrigation, CWSI can be used at vegetative or full vegetative stages next to NDVI or OSAVI depending on available resources.

Funding

This work was supported by the Innovation Laboratory for Small Scale Irrigation (ILSSI) project, funded by Feed the Future through the United States Agency for International Development (USAID), grant number: AID-OAA-A-13-0005. The donor supported on the initial stages of experimental design and infield data collection.

Declaration of Competing Interest

The authors declare that there are no financial conflict or personal relationships that could have appeared to influence the work reported in

this paper.

Acknowledgments

The authors would like to acknowledge support provided by Feed the Future Innovation Lab for Small Scale Irrigation through the U.S. Agency for International Development, under the terms of Contract No. AID-OAA-A-13-0005. The opinions expressed herein are those of the authors and do not necessarily reflect the views of the U.S. Agency for International Development. This work was also co-funded by the CGIAR Program on Water, Land, and Ecosystems (WLE). The authors are also thankful to the Sokoine University of Agriculture from Tanzania and the International Water Management Institute for their technical support. More gratitude goes to Prof. S.D. Tumbo for his contribution during proposal development, experimental design and set-up as well as data collection process. We would also like to give thanks to the Soil-Water Management Research Team from the Department of Engineering Sciences and Technology, under Prof. F.C. Kahimba for facilitating the the implementation of this research. Furthermore, the authors do acknowledge Mr. Justine Maisha and Ms. Mary Sauga for their tirelessly work during data collection.

References

Alvino, A., Marino, S., 2017. Remote sensing for irrigation of horticultural crops. Horticulturae 3 (2), 40. https://doi.org/10.3390/horticulturae3020040.

Badzmierowski, M.J., McCall, D.S., Evanylo, G., 2019. Using hyperspectral and multispectral indices to detect water stress for an urban turfgrass system. Agronomy 9 (8), 439. https://doi.org/10.3390/agronomy9080439.

Ballester, C., Brinkhoff, J., Quayle, W.C., Hornbuckle, J., 2019. Monitoring the effects of water stress in cotton using the green red vegetation index and red edge ratio. Remote Sens. 11 (7), 873. https://doi.org/10.3390/rs11070873.

Baluja, J., Diago, M.P., Balda, P., Zorer, R., Meggio, F., Morales, F., Tardaguila, J., 2012. Assessment of vineyard water status variability by thermal and multispectral imagery using an unmanned aerial vehicle (UAV). Irrig. Sci. 30 (6), 511–522. https://doi.org/10.1007/s00271-012-0382-9. 10.1007/s00271-012-0382-9.

Van Beek, J., Tits, L., Somers, B., Coppin, P., 2013. Stem water potential monitoring in pear orchards through WorldView-2 multispectral imagery. Remote Sens. 5 (12), 6647–6666. https://doi.org/10.3390/rs5126647.

Bellvert, J., Marsal, J., Girona, J., Zarco-Tejada, P.J., 2014. Seasonal evolution of crop water stress index in grapevine varieties determined with high-resolution remote sensing thermal imagery. Irrig. Sci. 33 (2), 81–93. https://doi.org/10.1007/s00271-014-0456-y.

Boyer, J., 1967. Leaf water potentials measured with a pressure chamber. Plant Physiol. 42 (1), 133–137. https://doi.org/10.1104/pp.42.1.133.

Chen, C., 2015. Determining the leaf emissivity of three crops by infrared thermometry. Sensors 15 (5), 11387–11401. https://doi.org/10.3390/s150511387.

Çolak, Y.B., Yazar, A., Çolak, İ., Akça, H., Duraktekin, G., 2015. Evaluation of crop water stress index (CWSI) for eggplant under varying irrigation regimes using surface and subsurface drip systems. Agric. Agric. Sci. Proc. 4, 372–382. https://doi.org/10.1016/j.aaspro.2015.03.042.

Damian, J.M., Pias, O.H.D.C., Cherubin, M.R., Fonseca, A.Z.D., Fornari, E.Z., Santi, A.L., 2020. Applying the NDVI from satellite images in delimiting management zones for annual crops. Sci. Agric. 77 (1) https://doi.org/10.1590/1678-992x-2018-0055.

Dave, C.P., Joshi, R., Srivastava, S.S., 2015. A survey on geometric correction of satellite imagery. Int. J. Comput. Appl. 116 (12), 24–27. https://doi.org/10.5120/20389-2655.

DeJonge, K.C., Taghvaeian, S., Trout, T.J., Comas, L.H., 2015. Comparison of canopy temperature-based water stress indices for maize. Agric. Water Manag. 156, 51–62. https://doi.org/10.1016/j.agwat.2015.03.023.

Diku, A., Bilena, H., Aadmir, S., 2015. Use of CROPWAT 8.0 program for the assessment of water demand of some agricultural crops in Albania. Int. J. Sci. 4 (09), 1–7. https://doi.org/10.18483/ijsci.817.

Enciso, J., Wiedenfeld, B., Jifon, J., Nelson, S., 2009. Onion yield and quality response to two irrigation scheduling strategies. Sci. Hortic. 120 (3), 301–305. https://doi.org/10.1016/j.scienta.2008.11.004.

Ge, Y., Bai, G., Stoerger, V., Schnable, J.C., 2016. Temporal dynamics of maize plant growth, water use, and leaf water content using automated high throughput RGB and hyperspectral imaging. Computers and Electronics in Agriculture 127, 625–632. https://doi.org/10.1016/j.compag.2016.07.028.

Genc, L., Inalpulat, M., Kizil, U., Mirik, M., Smith, S.E., Mendes, M., 2013. Determination of water stress with spectral reflectance on sweet corn (Zea mays L.) using classification tree (CT) analysis. Zemdirbyste-Agriculture 100 (1), 81–90. https://doi.org/10.13080/z-a.2013.100.011.

Gerhards, M., Rock, G., Schlerf, M., Udelhoven, T., 2016. Water stress detection in potato plants using leaf temperature, emissivity, and reflectance. Int. J. Appl. Earth Obs. Geoinf. 53, 27–39. https://doi.org/10.1016/j.jag.2016.08.004.

Goulden, M.L., Field, C.B., 1994. Three methods for monitoring the gas exchange of individual tree canopies: ventilated-chamber, sap-flow and Penman-Monteith measurements on evergreen oaks. Funct. Ecol. 8, 125–135. https://doi.org/10.2307/2390121.

Grant, O.M., Ochagavía, H., Baluja, J., Diago, M.P., Tardáguila, J., 2016. Thermal imaging to detect spatial and temporal variation in the water status of grapevine (Vitis vinifera L.). J. Hortic. Sci. Biotechnol. 91 (1), 43–54.

Gusso, A., 2018. Canopy temperatures distribution over soybean crop fields using satellite data in the Amazon biome frontier. Eur. J. Remote Sens. 51 (1), 901–910. https://doi.org/10.1080/22797254.2018.1511832.

Ihuoma, S.O., Madramootoo, C.A., 2019. Crop reflectance indices for mapping water stress in greenhouse grown bell pepper. Agric. Water Manag. 219, 49–58. https://doi.org/10.1016/j.agwat.2019.04.001.

Jones, H.G., Stoll, M., Santos, T., Sousa, C.D., Chaves, M.M., Grant, O.M., 2002. Use of infrared thermography for monitoring stomatal closure in the field: application to grapevine. J. Exp. Bot. 53 (378), 2249–2260. https://doi.org/10.1093/jxb/erf083.

Jorge, J., Vallbé, M., Soler, J.A., 2019. Detection of irrigation inhomogeneities in an olive grove using the NDRE vegetation index obtained from UAV images. Eur. J. Remote Sens. 52 (1), 169–177. https://doi.org/10.1080/22797254.2019.1572459.

Katsoulas, N., Elvanidi, A., Ferentinos, K.P., Kacira, M., Bartzanas, T., Kittas, C., 2016. Crop reflectance monitoring as a tool for water stress detection in greenhouses: a review. Biosyst. Eng. 151, 374–398. https://doi.org/10.1016/j.biosystemseng.2016.10.003.

Kyratzis, A.C., Skarlatos, D.P., Menexes, G.C., Vamvakousis, V.F., Katsiotis, A., 2017. Assessment of vegetation indices derived by UAV imagery for durum wheat phenotyping under a water limited and heat stressed mediterranean environment. Front. Plant Sci. 8, 1114. https://doi.org/10.3389/fpls.2017.01114.

Levy, D., Coleman, W.K., Veilleux, R.E., 2013. Adaptation of potato to water shortage: irrigation management and enhancement of tolerance to drought and salinity. Am. J. Potato Res. 90 (2), 186–206. https://doi.org/10.1007/s12230-012-9291-y.

Mandalu, M., Costa, T.H., 2018. Investigation on Tanzania's economic history since independence: the search for a development model. World J. Soc. Sci. Human. 4 (1), 61–68. (https://www.researchgate.net/publication/326508046_Investigation_on_Tanzania's_Economic_History_since_Independence_The_Search_for_a_Development_Model).

Maresma, Á., Ariza, M., Martínez, E., Lloveras, J., Martínez-Casasnovas, J.A., 2016. Analysis of vegetation indices to determine nitrogen application and yield prediction in maize (Zea mays L.) from a standard UAV service. Remote Sens. 8 (12), 973. https://doi.org/10.3390/rs8120973.

Mulla, D.J., 2013. Twenty-five years of remote sensing in precision agriculture: key advances and remaining knowledge gaps. Biosyst. Eng. 114 (4), 358–371. https://doi.org/10.1016/j.biosystemseng.2012.08.009.

P.R. Mwinuka, B.P. Mbilinyi, W.B. Mbungu, S.K. Mourice, H.F. Mahoo, P. Schmitter. Optimizing water and nitrogen application for neglected horticultural species in tropical sub-humid climate areas: A case of African eggplant (*Solanum aethiopicum* L.). Scientia Horticulturae, 276, 109756.

Naji, T.A., 2018. Study of vegetation cover distribution using DVI, PVI, WDVI indices with 2D-space plot. J. Phys. Conf. Ser. https://doi.org/10.1088/1742-6596/1003/1/012083.

Omer, G., Mutanga, O., Abdel-Rahman, E.M., Peerbhay, K., Adam, E., 2017. Mapping leaf nitrogen and carbon concentrations of intact and fragmented indigenous forest ecosystems using empirical modeling techniques and WorldView-2 data. ISPRS J. Photogramm. Remote Sens. 131, 26–39. https://doi.org/10.1016/j.isprsjprs.2017.07.005.

Patwardhan, A.S., Nieber, J.L., Johns, E.L., 1990. Effective rainfall estimation methods. J. Irrig. Drain. Eng. 116 (2), 182–193. https://doi.org/10.1061/(asce)0733-9437(1990)116:2(182).

Peng, D., Jiang, Z., Huete, A.R., Ponce-Campos, G.E., Nguyen, U., Luvall, J.C., 2013. Response of spectral reflectances and vegetation indices on varying juniper cone densities. Remote Sens. 5 (10), 5330–5345. https://doi.org/10.3390/rs5105330.

Petrie, P.R., Wang, Y., Liu, S., Lam, S., Whitty, M.A., Skewes, M.A., 2019. The accuracy and utility of a low cost thermal camera and smartphone-based system to assess grapevine water status. Biosyst. Eng. 179, 126–139. https://doi.org/10.1016/j.biosystemseng.2019.01.002.

Picoli, M.C.A., Duft, D.G., Machado, P.G., 2017. Identifying drought events in sugarcane using drought indices derived from Modis sensor. Pesqui. Agropec. Bras. 52 (11), 1063–1071. https://doi.org/10.1590/s0100-204×2017001100012.

Poblete-Echeverría, C., Espinace, D., Sepúlveda-Reyes, D., Zúñiga, M., Sanchez, M., 2017. Analysis of crop water stress index (CWSI) for estimating stem water potential in grapevines: comparison between natural reference and baseline approaches. Acta Hortic. 1150, 189–194. https://doi.org/10.17660/actahortic.2017.1150.27.

Prashar, A., Jones, H.G., 2014. Infra-red thermography as a high-throughput tool for field phenotyping. Agronomy 4 (3), 397–417. https://doi.org/10.3390/agronomy4030397.

Ranjan, R., Chandel, A.K., Khot, L.R., Bahlol, H.Y., Zhou, J., Boydston, R.A., Miklas, P.N., 2019. Irrigated pinto bean crop stress and yield assessment using ground based low altitude remote sensing technology. Inf. Process. Agric. 6 (4), 502–514. https://doi.org/10.1016/j.inpa.2019.01.005.

Reyes-González, A., Kjaersgaard, J., Trooien, T., Hay, C., Ahiablame, L., 2018. Estimation of crop evapotranspiration using satellite remote sensing-based vegetation index. Adv. Meteorol. 2018. https://doi.org/10.1155/2018/4525021.

Shiratsuchi, L., Ferguson, R., Shanahan, J., Adamchuk, V., Rundquist, D., Marx, D., Slater, G., 2011. Water and nitrogen effects on active canopy sensor vegetation indices. Agron. J. 103 (6), 1815–1826. https://doi.org/10.2134/agronj2011.0199.

Shi, X., Han, W., Zhao, T., Tang, J., 2019. Decision support system for variable rate irrigation based on UAV multispectral remote sensing. Sensors 19 (13), 2880. https://doi.org/10.3390/s19132880.

Siegfried, J., Longchamps, L., Khosla, R., 2019. Multispectral satellite imagery to quantify in-field soil moisture variability. J. Soil Water Conserv. 74 (1), 33–40. https://doi.org/10.2489/jswc.74.1.33.

Soulis, K.X., Elmaloglou, S., Dercas, N., 2015. Investigating the effects of soil moisture sensors positioning and accuracy on soil moisture based drip irrigation scheduling systems. Agric. Water Manag. 148, 258–268. https://doi.org/10.1016/j.agwat.2014.10.015.

Stone, K.C., Bauer, P.J., Sigua, G.C., 2016. Irrigation management using an expert system, soil water potentials, and vegetative indices for spatial applications. Trans. ASABE 59 (3), 941–948. https://doi.org/10.13031/trans.59.11550.

Ustuner, M., Sanli, F.B., Abdikan, S., Esetlili, M.T., Kurucu, Y., 2014. Crop type classification using vegetation indices of rapideye imagery. Int. Arch. Photogramm. Remote Sens. SpatialInf. Sci. 40 (7), 195. https://doi.org/10.5194/isprsarchives-xl-7-195-2014. 10.5194/isprsarchives-xl-7-195-2014.

Veysi, S., Naseri, A.A., Hamzeh, S., Bartholomeus, H., 2017. A satellite based crop water stress index for irrigation scheduling in sugarcane fields. Agric. Water Manag. 189, 70–86. https://doi.org/10.1016/j.agwat.2017.04.016.

Wuyts, M., Kilama, B., 2014. Economic transformation in Tanzania: Vicious or virtuous Circle?. (Accessed 14 July 2020).

Xue, J., Su, B., 2017. Significant remote sensing vegetation indices: a review of developments and applications. J. Sens. 2017 https://doi.org/10.1155/2017/1353691.

Yonah, I.B., Mourice, S.K., Tumbo, S.D., Mbilinyi, B.P., Dempewolf, J., 2018. Unmanned aerial vehicle-based remote sensing in monitoring smallholder, heterogeneous crop fields in Tanzania. Int. J. Remote Sens. 39 (15–16), 5453–5471. https://doi.org/10.1080/01431161.2018.1455241.

Zhang, F., Zhou, G., 2019. Estimation of vegetation water content using hyperspectral vegetation indices: a comparison of crop water indicators in response to water stress treatments for summer maize. BMC Ecol. 19 (1), 18. https://doi.org/10.1186/s12898-019-0233-0.

Zhao, Y., Potgieter, A.B., Zhang, M., Wu, B., Hammer, G.L., 2020. Predicting wheat yield at the field scale by combining high-resolution Sentinel-2 satellite imagery and crop modelling. Remote Sens. 12 (6), 1024. https://doi.org/10.3390/rs12061024.

Zotarelli, L., Dukes, M.D., Scholberg, J.M.S., Femminella, K., Munoz-Carpena, R., 2011. Irrigation scheduling for green bell peppers using capacitance soil moisture sensors. J. Irrig. Drain. Eng. 137 (2), 73–81. https://doi.org/10.1061/(asce)ir.1943-4774.0000281.

Zou, X., Mõttus, M., 2017. Sensitivity of common vegetation indices to the canopy structure of field crops. Remote Sens. 9 (10), 994. https://doi.org/10.3390/rs9100994.